

Enhancement of Magnon Transport by Superconductor Meissner Screening

Xi-Han Zhou,¹ Xiyin Ye,¹ Lihui Bai,² and Tao Yu^{1,*}

¹*School of Physics, Huazhong University of Science and Technology, Wuhan 430074, China*

²*School of Physics, State Key Laboratory of Crystal Materials, Shandong University, Jinan, 250100 China*

(Dated: April 4, 2024)

Recent experiments observe the spin-wave-Meissner-current modes in ferromagnetic insulator-superconductor heterostructures, in which the coherently excited spin waves seemingly do not decay as usual beneath the superconductor strip [Borst *et al.*, *Science* **382**, 430 (2023)]. We interpret this phenomenon by demonstrating that the stray magnetic field emitted by the magnetization dynamics is reflected, focused, and *enhanced* inside the ferromagnet by the supercurrent induced in the superconductor, such that the group velocity of spin waves is strongly enhanced. Analytical and numerical calculations based on this model predict that the coherent transport of magnons is enhanced by close to 500% for yttrium iron garnet capped by superconducting NbN with a decay length exceeding millimeters. Our finding may augment the performance of magnons in quantum information and quantum transport processing.

Introduction.—Spin waves or their quanta, magnons, are collective excitations of ordered magnetic moments, which can strongly hybridize with other degrees of freedom for classical information transduction, quantum information processing, and long-range pure-spin transport [1, 3–9, 32]. In various magnonic devices, the intrinsic damping of spin waves is detrimental to their transport since it limits their possible propagation length, usually much smaller than photons and phonons. Ferrimagnetic insulator yttrium iron garnet (YIG) is currently the best material for magnon transport due to its record low damping [10–13], long characteristic decay length of tens of micrometers [11, 13, 14], and narrowest known linewidth of ferromagnetic resonance, resulting in a lifetime of a few hundred nanoseconds [15, 16]. In spite of these merits, their dissipation parameters nowadays severely limit the appeal of employing magnons in the quantum information [8, 9, 17–22] and quantum transport and appear to be challenging to be further improved via optimizing the crystal quality.

Superconducting devices are instruments implemented to avoid Ohmic dissipation and thereby employed on purpose in superconducting spintronics [23–27], quantum information [17–21, 28–30], and topological computation [31]. Useful ferromagnet and superconductor heterostructure are pursued to transport spin information without dissipation and realize new functionalities [23–27, 32]. Superconductors with thicknesses comparable to London’s penetration depth allow the penetration of stray field emitted by spin waves, providing the electromotive force that drives the supercurrent and in turn, causes the Osted magnetic field that shifts the spin-wave frequency by many gigahertz [33–46]. However, the role of dissipationless supercurrent on magnon transport via this “gating” effect has not yet been explored in previous theories [33–46], raising the question that whether the supercurrent can “shortcut” the magnon energy flow as in electronics.

Borst *et al.* recently observed hybridized spin-wave-

Meissner-current modes showing a modulated spin wavelength in the ferromagnetic insulator(FI)-superconductor (SC) heterostructures [35]. This experiment also finds that the coherently excited spin waves seemingly do not decay as usual beneath the superconductor strip with a significant enhancement of propagation length. It was speculated to be an artifact that an additional current may be induced in the SC strip when excited by the nearby microwave antenna [35]. Less attention was, however, paid to the possible role of the supercurrent on the magnon transport in the FI-SC heterostructures.

In this Letter, we propose to use SCs for a local and unidirectional enhancement of magnon transport in thin FI by its inductive coupling to the Cooper-pair supercurrent as in Fig. 1. We find that the electromotive force

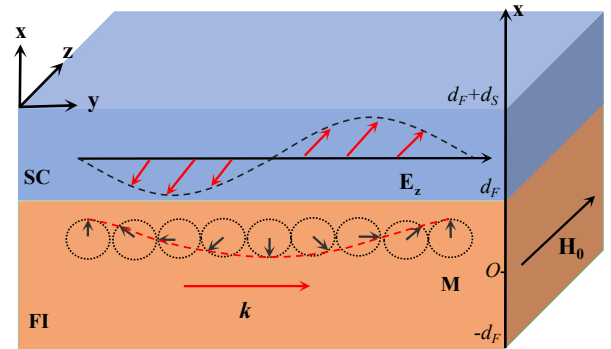


FIG. 1. Inductive coupling between magnetization dynamics and Cooper-pair supercurrent in FI-SC heterostructure. An in-plane external magnetic field \mathbf{H}_0 biases \mathbf{M}_0 to the \hat{z} -direction. Spin waves propagating normally to the saturated magnetization \mathbf{M}_0 radiate the electric fields along \mathbf{M}_0 . An inserted thin insulator spacer is assumed to suppress the exchange proximity effect.

and supercurrent induced by the stray magnetic fields emitted by the magnetization dynamics can reflect, focus, and enhance the stray field inside the FI, such that the group velocity of spin waves is significantly enhanced,

while the net damping is not suppressed. We predict that by changing the temperature across the superconducting transition temperature (*e.g.*, 5-10 K for NbN [47–49]), the magnon transport can be unidirectionally enhanced by up to 450% for YIG film capped by superconducting NbN film, rendering a decay length exceeding millimeters, well beyond the present records [10–14]. Since quantum transport and quantum information are performed at cryogenic temperatures, our findings may augment the performance of magnons in these fields.

Reflection of magnetization radiation by proximity superconductors.—Here we analytically calculate the electric and magnetic fields radiated by the magnetization fluctuation in the FI-SC heterostructure by solving Maxwell’s equations and matching the boundary conditions at interfaces between the FI, SC, and vacuum. As shown in Fig. 1, a static in-plane magnetic field \mathbf{H}_0 orients the saturated magnetization \mathbf{M}_0 to the $\hat{\mathbf{z}}$ -direction and the thickness of FI and SC are $2d_F$ and d_S , respectively. For the transverse magnetization fluctuation $M_{x,y}(\mathbf{r}, t) = \mathcal{M}_{x,y}(x)e^{i\mathbf{k}\cdot\boldsymbol{\rho}}e^{-i\omega t}$ of frequency ω with amplitudes $\mathcal{M}_{x,y}$ and wave vector $\mathbf{k} = (0, k_y, k_z)$ propagating in the film plane $\boldsymbol{\rho} = y\hat{\mathbf{y}} + z\hat{\mathbf{z}}$, $\mathcal{M}_{x,y}$ is nearly uniform across the film normal direction (*i.e.*, the $\hat{\mathbf{x}}$ -direction) when the film is sufficiently thin and the wavelength of spin waves ($\gg 2d_F$) is long [10–14, 35]. Such magnetic fluctuation radiates the electric field $\mathbf{E}(\mathbf{r}, t)$ via the magnetization current $\mathbf{J}_M(\mathbf{r}, t) = \nabla \times \mathbf{M}(\mathbf{r}, t)$. According to Maxwell’s equations [50], the radiation obeys $\nabla^2 \mathbf{E}(\mathbf{r}, t) + k_0^2 \mathbf{E}(\mathbf{r}, t) = -i\omega\mu_0 \mathbf{J}_M(\mathbf{r}, t)$, where $k_0 = \omega\sqrt{\mu_0\varepsilon_0}$ with μ_0 and ε_0 being the vacuum permeability and permittivity, respectively.

The amplitudes $i\mathcal{M}_x = a_{\mathbf{k}}\mathcal{M}_y$ describe the ellipticity of spin waves in terms of $a_{\mathbf{k}}$. $a_{\mathbf{k}} = 1$ indicates the circular polarization, while the magnetic stray field renders $a_{\mathbf{k}} \neq 1$. Analyzing the radiated electric fields by a single FI helps to understand the role of the capped SCs. We find the electric fields emitted by a single ferromagnetic film

$$\mathbf{E}^{(0)}(\mathbf{r}, t) = \boldsymbol{\mathcal{E}}^{(0)}(x)e^{i\mathbf{k}\cdot\boldsymbol{\rho} - i\omega t}, \quad (1)$$

governed by the amplitudes

$$\boldsymbol{\mathcal{E}}_{x/y}^{(0)} = +(-)\frac{\omega\mu_0\mathcal{M}_{y/x}k_z}{2\mathcal{A}_k^2} \begin{cases} \alpha_k(x), & x > d_F \\ -2 + \delta_+(k, x), & |x| \leq d_F \\ -\alpha_k^*(x), & x < -d_F \end{cases},$$

$$\boldsymbol{\mathcal{E}}_z^{(0)} = \frac{\omega\mu_0\mathcal{M}_y}{2\mathcal{A}_k} \begin{cases} (\beta_k - 1)\alpha_k(x), & x > d_F \\ (\delta_+(k, x) - 2)\beta_k + \delta_-(k, x), & |x| \leq d_F \\ (\beta_k + 1)\alpha_k^*(x), & x < -d_F \end{cases},$$

where $\mathcal{A}_k = \sqrt{k_0^2 - k^2} \rightarrow ik$, $\alpha_k(x) = e^{i\mathcal{A}_k(x+d_F)} - e^{i\mathcal{A}_k(x-d_F)}$, $\delta_{\pm}(k, x) = e^{-i\mathcal{A}_k(x-d_F)} \pm e^{i\mathcal{A}_k(x+d_F)}$, and $\beta_{\mathbf{k}} = -ia_{\mathbf{k}}k_y/\mathcal{A}_k \rightarrow -a_{\mathbf{k}}k_y/k$. When the spin waves propagate normally to \mathbf{M}_0 , the electric field is linearly polarized along the saturated magnetization $\hat{\mathbf{z}}$ -direction

since $\boldsymbol{\mathcal{E}}_{x/y}^{(0)}$ vanishes when $k_z = 0$. Particularly, for circularly polarized spin waves with $a_{\mathbf{k}} = 1$, $\beta_{\mathbf{k}} \sim -a_{\mathbf{k}}k_y/k = -\text{sgn}(k_y)$ depends on the propagation direction: above (below) the ferromagnetic film, the electric field exists only when $k_y > 0$ ($k_y < 0$), governed by the attenuation length $|k_y|^{-1}$, but vanishes when $k_y < 0$ ($k_y > 0$).

We then demonstrate that the radiated electric (and magnetic) field by a single FI is strongly reflected, focused, and enhanced by the adjacent SCs. Inside the SCs, the electric field is screened via $\nabla^2 \mathbf{E}(\mathbf{r}, t) + k_s^2 \mathbf{E}(\mathbf{r}, t) = 0$, where $k_s = \sqrt{\omega^2\mu_0\varepsilon_0 - 1/\lambda_L^2}$ is the electromagnetic wave number in the SC, which is approximately purely imaginary and governed by the inverse London’s penetration depth λ_L [50]. Therefore, the electric field is screened by the supercurrent and penetrates only within λ_L . The temperature T affects the penetration according to $\lambda_L(T) = \lambda_L(T = 0 \text{ K})/\sqrt{1 - (T/T_c)^4}$ [51], which is large when T approaches the superconducting transition temperature T_c .

The boundary condition governs the reflection and transmission of electric fields at interfaces. The in-plane $\mathbf{E}_{\parallel}(\mathbf{r}, t)$ is continuous at interfaces [50]. For the normal component E_x , there is no charge accumulation inside SCs at microwave frequency, such that $\nabla \cdot \mathbf{E}(\mathbf{r}, t) = 0$ in it. On the other hand, $\partial_{\parallel} \mathbf{E}_{\parallel}(\mathbf{r}, t)$ is continuous, and thereby, combining with $\nabla \cdot \mathbf{E}(\mathbf{r}, t) = 0$, $\partial_x E_x(\mathbf{r}, t)$ is continuous at interfaces. Finally, the current $J_x(\mathbf{r}, t) + \varepsilon_0 \partial_t E_x(\mathbf{r}, t)$ is continuous at interfaces due to the charge conservation. Carefully matching the boundary conditions refine the previous theoretical treatments [33, 35], by which we obtain the electric field for all wave vectors \mathbf{k} , referring to the Supplemental Material for details [52].

Here, we focus on the Damon-Eshbach (DE) configuration with $k_z = 0$ since these spin waves are modulated most strongly by SCs and were recently measured [35]. In this case, as that radiated by a single FI (1) only the electric field $E_z \hat{\mathbf{z}} \parallel \mathbf{M}_0$ exists, as addressed in Fig. 1. The electric field emitted by a single FI (1) is reflected by the SC according to the wave-number dependent reflection coefficient

$$\mathcal{R}_k = (\mathcal{A}_k - \mathcal{B}_k)/(\mathcal{A}_k + \mathcal{B}_k), \quad (2)$$

where $\mathcal{B}_k = \sqrt{k_s^2 - k^2}$ and $k = |k_y|$ in the DE configuration, such that inside the FI

$$E_z(\mathbf{r}, t) = E_z^{(0)}(\mathbf{r}, t) + \mathcal{R}_k E_z^{(0)}(\mathbf{r}, t)|_{x=d_F} e^{-i\mathcal{A}_k(x-d_F)}. \quad (3)$$

For a large $k \gg \lambda_L^{-1}$, the electric field rapidly decays within the decay length $k^{-1} \ll \lambda_L$, such that $|\mathcal{A}_k| \sim |\mathcal{B}_k|$, implying the vanished reflection (2) $\mathcal{R}_k \sim (\mathcal{A}_k - \mathcal{A}_k)/(2\mathcal{A}_k) \rightarrow 0$, *i.e.*, the SC hardly affects the spin waves. On the other hand, when $k \ll \lambda_L^{-1}$, $|\mathcal{A}_k| \ll |\mathcal{B}_k|$ and $\mathcal{R}_k \sim -\mathcal{B}_k/\mathcal{B}_k \rightarrow -1$, such that the electric field is totally reflected by the SC with a π phase shift, resulting in no net supercurrents driven inside the SC,

i.e., the magnon and Cooper-pair supercurrent decouples. Thereby, only the spin waves with $k \sim \lambda_L^{-1}$ are most strongly modulated by the SCs.

The electric field (3) induces the magnetic field $\mathbf{H}_d(\mathbf{r}, t)$ according to Faraday's Law $i\omega\mu_0[\mathbf{H}_d(\mathbf{r}, t) + \mathbf{M}(\mathbf{r}, t)] = \nabla \times \mathbf{E}(\mathbf{r}, t)$ [50]. As addressed before, the magnetic fluctuation is nearly uniform across the thin FI, and we thereby take the spatial average for the stray field along the \hat{x} -direction:

$$\begin{aligned}
H_{d,y} &= M_y(P_k e^{-kd_F} - 1) \\
&+ \mathcal{R}_k M_y P_k e^{-kd_F} (1 - e^{-2kd_F}) \frac{1 + a_{k_y} \text{sgn}(k_y)}{2} \\
&\equiv \kappa_y(k_y) M_y, \\
H_{d,x} &= -M_x P_k e^{-kd_F} \\
&+ \mathcal{R}_k M_x P_k e^{-kd_F} (1 - e^{-2kd_F}) \frac{1 + a_{k_y}^{-1} \text{sgn}(k_y)}{2} \\
&\equiv \kappa_x(k_y) M_x,
\end{aligned} \tag{4}$$

where the form factor $P_k = \sinh(kd_F)/(kd_F)$. As in the electric field (3), the dipolar field is also expressed as the one radiated by a single FI superposed by that reflected by the SCs. When $k_y \rightarrow 0$ or $\mathcal{R}_k \rightarrow 0$, the influence of the SC vanishes, and the dipolar field recovers to that of a single FI, which, however, is *enhanced* when $\mathcal{R}_k \rightarrow -1$ assuming $a_{k_y} \sim 1$. The dimensionless factors $\kappa_y(k_y) < 0$ and $\kappa_x(k_y) < 0$ are generally enhanced *in magnitude* by the SC. The chirality of the dipolar field is now clear: for circularly polarized spin waves with $a_{k_y} \rightarrow 1$, $[1 + a_{k_y} \text{sgn}(k_y)]/2 \rightarrow 0$ and $[1 + a_{k_y}^{-1} \text{sgn}(k_y)]/2 \rightarrow 0$ when $k_y < 0$, but becomes unity when $k_y > 0$.

We now illustrate the effect of SCs on the stray field by comparing it with that of an isolated FI in Fig. 2(a) and (b). We take $d_F = 50$ nm, $d_S = 300$ nm, and London's penetration depth $\lambda_L = 80$ nm at $T = 1.2$ K $\sim 0.1T_c$ for NbN [47–49]. For the spin wave with $k_y = 4 \mu\text{m}^{-1}$, without gating its stray field mainly exists above the ferromagnetic film $x > 0$ [Fig. 2(a)]. When in proximity to the SC, the magnetic field at $x > 0$ is reflected and decays faster inside the SC, which is then enhanced inside the ferromagnetic film. In the present case, the enhancement is up to 30% compared to that with a single FI. By contrast, when $k_y = -4 \mu\text{m}^{-1}$, as shown in Fig. 2(b), the emitted magnetic field without gating mainly exists below the ferromagnetic film $x < 0$, thereby is hardly affected by the SC fabricated at $x > 0$.

The selective enhancement of stray field is governed by the general symmetry principle for the system with translation invariance: as shown in Fig. 2(c) and (d) the capped SC breaks the twofold-rotation symmetry around the saturated magnetization but retains the mirror symmetry with the mirror plane normal to the saturated magnetization.

Modulated dispersion, group velocity, lifetime, and ellipticity of spin waves.—Such selectively enhanced dipole-

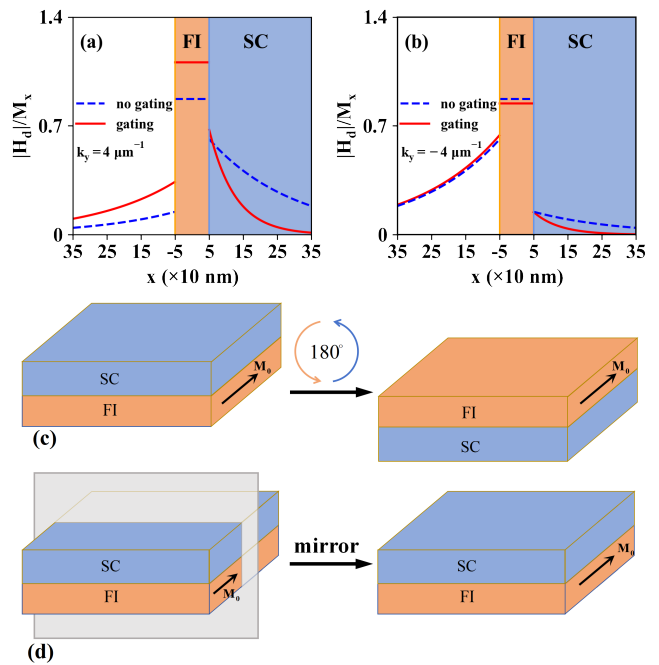


FIG. 2. Selective enhancement of radiated magnetic field by proximity SCs with $k_y = 4 \mu\text{m}^{-1}$ [(a)] and $k_y = -4 \mu\text{m}^{-1}$ [(b)]. The blue dotted curve plots the magnetic field of an isolated FI with thickness $2d_F = 100$ nm. The red curve illustrates the magnetic field of the FI-SC heterostructure with SC thickness $d_S = 300$ nm and penetration depth $\lambda_L = 80$ nm. (c) and (d) show the SC-FI heterostructure with twofold rotation symmetry breaking and mirror symmetry.

lar field (4) strongly affect the magnetization dynamics. In the Landau-Lifshitz-Gilbert (LLG) equation $\partial_t \mathbf{M} = -\mu_0 \gamma \mathbf{M} \times \mathbf{H}_{\text{eff}} + \alpha_G \mathbf{M}/M_0 \times \partial_t \mathbf{M}$, γ is the gyromagnetic ratio, α_G is the Gilbert damping constant, and the effective magnetic field \mathbf{H}_{eff} includes the static field $\mathbf{H}_0 = H_0 \hat{z}$, the dipolar field \mathbf{H}_d (4), and the exchange field $\mathbf{H}_{\text{ex}} = \alpha_{\text{ex}} \nabla^2 \mathbf{M}$ with the exchange stiffness α_{ex} . The damping term contributes to an extra imaginary component in the eigenfrequency, i.e., $\tilde{\omega}_{\mathbf{k}} = \omega_{\mathbf{k}} - i\Gamma_{\mathbf{k}}$. With $\{M_x, M_y\} \propto e^{-i\tilde{\omega}_{\mathbf{k}} t}$, we find the eigenfrequency, inverse lifetime, and ellipticity of the collective modes

$$\omega(k_y) = \mu_0 \gamma \sqrt{(H_{k_y} - \kappa_x(k_y) M_0)(H_{k_y} - \kappa_y(k_y) M_0)}, \tag{5a}$$

$$\Gamma(k_y) = \frac{\mu_0 \gamma \alpha_G}{2} [2H_{k_y} - M_0 (\kappa_x(k_y) + \kappa_y(k_y))], \tag{5b}$$

$$a(k_y) = \sqrt{(H_{k_y} - \kappa_x(k_y) M_0)/(H_{k_y} - \kappa_y(k_y) M_0)}, \tag{5c}$$

where $H_{k_y} = H_0 + \alpha_{\text{ex}} k_y^2 M_0$. Equation (5c) provides the self-consistent equation for solving the ellipticity, with which we numerically find the dispersion (5a) and inverse lifetime (5b). When $k_y > 0$, $\kappa_x(k_y) < 0$ and $\kappa_y(k_y) < 0$ are both enhanced in magnitude by the adjacent SC, such that both the frequency (5a) and the inverse lifetime (5b)

are enhanced. It is then not clear whether the transport can be definitely enhanced or not.

Enhancement of magnon transport.—We then turn to calculate the characteristic decay length of the gated spin waves when excited by an external Oersted magnetic field $\mathbf{h}(\mathbf{r}, t)$ of frequency Ω , emitted from a long stripline along the saturated magnetization $\hat{\mathbf{z}}$ -direction, similar to the configuration in the experiments [13, 35]. It couples with the transverse magnetization via the Zeeman interaction [53] $\hat{H}_{\text{int}} = -\mu_0 \int \mathbf{M}(\mathbf{r}) \cdot \mathbf{h}(\mathbf{r}, t) d\mathbf{r}$. According to the linear response theory, the excited magnetization by the Fourier components $h_\beta(x, k_y, \Omega) = (1/L) \int dy e^{-ik_y y} h_\beta(y)$, where L is the sample length, of such field reads

$$M_\alpha(x, k_y, \Omega) = \mu_0 (\gamma \hbar)^2 \int_{-d_F}^{d_F} dx' \chi_{\alpha\beta}(x, x', k_y, \Omega) \times h_\beta(x', k_y, \Omega), \quad (6)$$

where the spin susceptibility

$$\chi_{\alpha\beta}(x, x', \mathbf{k}, \omega) = -\frac{2M_0}{\gamma \hbar^2} \mathcal{M}_\alpha^{\mathbf{k}}(x) \mathcal{M}_\beta^{\mathbf{k}*}(x') \frac{1}{\Omega - \tilde{\omega}_{\mathbf{k}}}. \quad (7)$$

Here the normalized amplitude of the modes [54, 55]

$$\mathcal{M}_y^{\mathbf{k}} = \frac{1}{2\sqrt{2d_F}} \frac{1}{\sqrt{a_{\mathbf{k}}}}, \quad \mathcal{M}_x^{\mathbf{k}} = -\frac{i}{2\sqrt{2d_F}} \sqrt{a_{\mathbf{k}}}.$$

After summation over the Fourier components, the excited magnetization in the real space

$$M_\alpha(y, t) = \sum_{k_y} e^{ik_y y} M_\alpha(k_y, t) = 4iL\mu_0\gamma d_F M_0 \times \mathcal{M}_\alpha^{k_\Omega} \mathcal{M}_\beta^{k_\Omega*} \frac{1}{v_{k_\Omega}} e^{i(k_\Omega y - \Omega t)} e^{-\tilde{k}_\Omega y} h_\beta(k_\Omega), \quad (8)$$

where $\tilde{k}_y = k_\Omega + i\tilde{k}_\Omega$ is the positive root of $\tilde{\omega}(\tilde{k}_y) = \Omega$ and $v_{\mathbf{k}} = \partial\omega(\mathbf{k})/\partial\mathbf{k}$ is the group velocity of spin waves. $\lambda = 1/\tilde{k}_\Omega$ governs the decay length of the excited magnetization.

We find \tilde{k}_Ω as follows. Since $\tilde{\omega}(k_y)$ is solved from the linearized LLG equation, $\tilde{\omega}(k_y) = \Omega$ obeys

$$\begin{aligned} \Omega^2 &= [\mu_0\gamma(H_{k_y} - M_0\kappa_y(k_y)) - i\Omega\alpha_G] \\ &\times [(\mu_0\gamma(H_{k_y} - M_0\kappa_x(k_y)) - i\Omega\alpha_G)] \\ &= \omega^2(k_y) - 2i\Omega\Gamma(k_y). \end{aligned} \quad (9)$$

The solution $\tilde{k}_y = k_\Omega + i\tilde{k}_\Omega$ is a complex number containing a small imaginary component $\tilde{k}_\Omega \ll k_\Omega$, which allows us to expand $\omega(k_y)$ to the leading order as

$$\omega(\tilde{k}_y) = \omega(k_\Omega) + v_{k_\Omega} i\tilde{k}_\Omega. \quad (10)$$

Substituting Eq. (10) into (9) and equating the real and imaginary parts of Eq. (9) lead to $\Omega = \omega(k_\Omega)$ and $\tilde{k}_\Omega = \Gamma(k_\Omega)/v_{k_\Omega}$. So the characteristic decay length

$$\lambda = 1/\tilde{k}_\Omega = v_{k_\Omega}/\Gamma(k_\Omega) = v_{k_\Omega}\tau(k_\Omega) \quad (11)$$

is simply governed by the group velocity and the magnon lifetime $\tau(k) = 1/\Gamma(k)$.

Figure 3 plots the modulated properties of spin waves by the adjacent SC in the DE configuration $\mathbf{k} \perp \mathbf{M}_0$. In

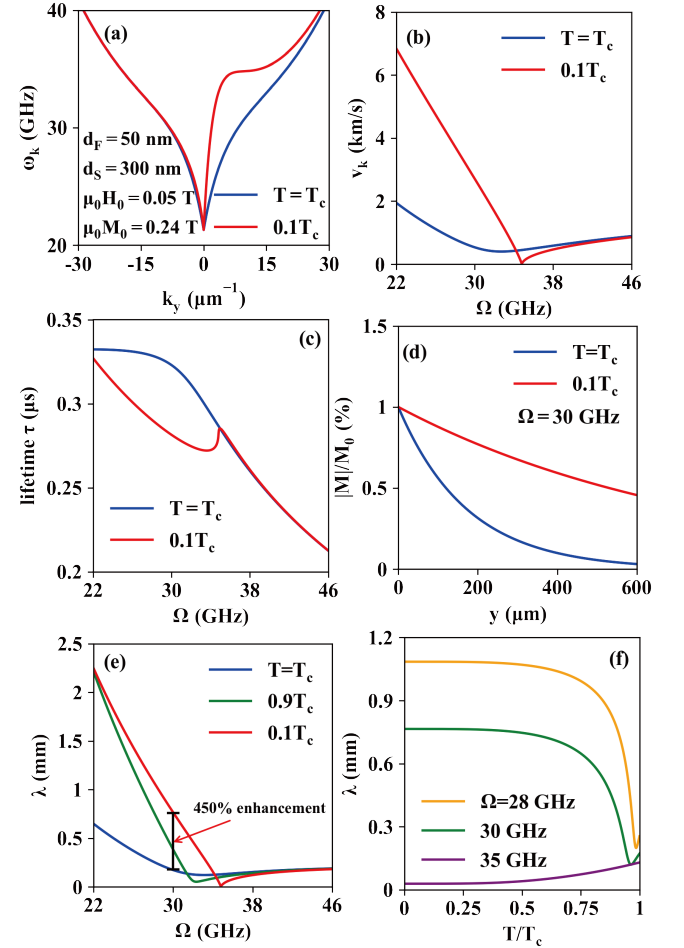


FIG. 3. Enhancement of magnon transport in FI by an adjacent SC in the DE configuration $\mathbf{k} \perp \mathbf{M}_0$. (a), (b), and (c) plot the frequency shift, enhanced group velocity, and lifetime of magnons when the temperature is decreased from $T = T_c$ to $0.1T_c$. These modulations by the adjacent SC lead to a significant enhancement of magnon transport as demonstrated in the dependencies of the characteristic decay length on the space [(d)], excited frequency Ω [(e)], and temperatures [(f)].

the calculation, we take the YIG film of thickness $2d_F = 100$ nm, saturated magnetization $\mu_0 M_0 = 0.24$ T [35, 56], exchange stiffness $\alpha_{\text{ex}} = 3 \times 10^{-16}$ m², and damping coefficient $\alpha_G = 10^{-4}$ [16], biased by the in-plane field $\mu_0 H_0 = 0.05$ T. We use the superconducting NbN of thickness $d_S = 300$ nm and London's penetration depth $\lambda_L = 80$ nm at $T = 0.1T_c = 1.2$ K [47–49]. Comparing the dispersions at $T = 0.1T_c$ and T_c , Fig. 3(a) shows decreasing the temperature, the magnon dispersion is strongly shifted upwards only when $k_y > 0$. There is no frequency shift at the ferromagnetic resonance $k_y = 0$ due to the total reflection of stray fields by the SC, and the

shift vanishes when the wave vector is large since the exchange interaction dominates. The frequency shift is then largest when $k_y \sim \lambda_L^{-1}$, resulting in the non-monotonic modulation of the group velocity as in Fig. 3(b): the group velocity is strongly enhanced (slightly suppressed) when $k_y \in [0, \lambda_L^{-1}]$ ($k_y \gtrsim \lambda_L^{-1}$). Furthermore, the lifetime of magnons is not suppressed, as shown in Fig. 3(c).

According to Eq. (11), the group velocity and lifetime of magnons jointly govern their characteristic decay length. As plotted in Fig. 3(e), when decreasing the temperature from $T = T_c$ to $0.1T_c$, the decay of the excited magnetization becomes much slower due to the screening of the stray field by SCs. Figure 3(d) and (f) plot the sharp dependencies of decay length on excited frequencies Ω and temperatures, in which we find the SC generally enhances the magnon transport when the excited wave vector $k_y \lesssim \lambda_L^{-1}$. Particularly, we estimate the enhancement for YIG can be as large as 450%, resulting in the decay length exceeding millimeters at lower frequencies.

Conclusion and discussion.—In conclusion, we develop the model calculations of the inductive interaction between magnons and SC supercurrent and predict an efficient approach to unidirectionally enhance the transport of magnons in the microwave frequencies even in the best ferrimagnet YIG via the screening of its dynamical stray field by adjacent SCs. Such mechanism is free of charge and spin-orbit-coupling, thereby also suitable for the metallic ferromagnet [57]. The frequency of some antiferromagnets [58, 59] lies in the control window as well. At room temperature, the associated mechanism relies on the perfect diamagnetism of conventional SCs for microwaves, which may be replaceable by other materials with large diamagnetic susceptibilities [60, 61]. Our finding may stimulate explorations of magnon on-chip quantum information and transport in the context of superconducting magnonics.

This work is financially supported by the National Key Research and Development Program of China under Grant No. 2023YFA1406600, the National Natural Science Foundation of China under Grants No. 12374109 and No. 12274260, as well as the startup grant of Huazhong University of Science and Technology. We thank Toeno van der Sar, Gerrit Bauer, and Yafei Ren for the useful discussions.

* taoyuphy@hust.edu.cn

- [1] B. Lenk, H. Ulrichs, F. Garbs, and M. Münzenberg, The building blocks of magnonics, *Phys. Rep.* **507**, 107 (2011).
- [2] A. V. Chumak, V. I. Vasyuchka, A. A. Serga, and B. Hillebrands, Magnon spintronics, *Nat. Phys.* **11**, 453 (2015).
- [3] L. J. Cornelissen, J. Liu, R. A. Duine, J. Ben Youssef, and B. J. van Wees, Long-distance transport of magnon spin information in a magnetic insulator at room temperature, *Nat. Phys.* **11**, 1022 (2015).
- [4] D. Grundler, Nanomagnonics around the corner, *Nat. Nanotechnol.* **11**, 407 (2016).
- [5] V. E. Demidov, S. Urazhdin, G. de Loubens, O. Klein, V. Cros, A. Anane, and S. O. Demokritov, Magnetization oscillations and waves driven by pure spin currents, *Phys. Rep.* **673**, 1 (2017).
- [6] A. Brataas, B. van Wees, O. Klein, G. de Loubens, and M. Viret, Spin Insulatronics, *Phys. Rep.* **885**, 1 (2020).
- [7] A. Barman, G. Gubbiotti, S. Ladak, A. O. Adeyeye, M. Krawczyk, J. Gräfe, C. Adelman, S. Cotofana, A. Naeemi, V. I. Vasyuchka *et al.*, The 2021 magnonics roadmap, *J. Phys.: Condens. Matter* **33**, 413001 (2021).
- [8] T. Yu, Z. C. Luo, and G. E. W. Bauer, Chirality as generalized spin-orbit interaction in spintronics, *Phys. Rep.* **1009**, 1 (2023).
- [9] B. Flebus, S. Rezendé, D. Grundler, and A. Barman, Recent advances in magnonics, *J. Appl. Phys.* **133**, 160401 (2023).
- [10] V. Cherepanov, I. Kolokolov, and V. L'vov, The saga of YIG: Spectra, thermodynamics, interaction and relaxation of magnons in a complex magnet, *Phys. Rep.* **229**, 81 (1993).
- [11] A. A. Serga, A. V. Chumak, and B. Hillebrands, YIG magnonics, *J. Phys. D* **43**, 264022 (2010).
- [12] M. Wu and A. Hoffmann, *Recent Advances in Magnetic Insulators: From Spintronics to Microwave Applications* (Elsevier, Amsterdam, 2013), Vol. 64.
- [13] C. P. Liu, J. L. Chen, T. Liu, F. Heimbach, H. M. Yu, Y. Xiao, J. F. Hu, M. C. Liu, H. C. Chang, T. Stueckler, S. Tu, Y. G. Zhang, Y. Zhang, P. Gao, Z. M. Liao, D. P. Yu, K. Xia, N. Lei, W. S. Zhao, and M. Z. Wu, Long-distance propagation of short-wavelength spin waves, *Nat. Commun.* **9**, 738 (2018).
- [14] X.-Y. Wei, O. A. Santos, C. H. S. Lusero, G. E. W. Bauer, J. Ben Youssef, and B. J. van Wees, Giant magnon spin conductivity in ultrathin yttrium iron garnet films, *Nat. Mater.* **21**, 1352 (2022).
- [15] T. Makiuchi, T. Hioki, H. Shimizu, K. Hoshi, M. Elyasi, K. Yamamoto, N. Yokoi, A. A. Serga, B. Hillebrands, G. E. W. Bauer, and E. Saitoh, Persistent magnetic coherence in magnets, *Nat. Mat.* (2024).
- [16] H. Chang, P. Li, W. Zhang, T. Liu, A. Hoffmann, L. Deng, and M. Wu, *IEEE Magn. Lett.* **5**, 6700104 (2014).
- [17] Y. Tabuchi, S. Ishino, A. Noguchi, T. Ishikawa, R. Yamazaki, K. Usami, and Y. Nakamura, Coherent coupling between a ferromagnetic magnon and a superconducting qubit, *Science* **349**, 405 (2015).
- [18] D. L. Quirion, S. P. Wolski, Y. Tabuchi, S. Kono, K. Usami, and Y. Nakamura, Entanglement-based single-shot detection of a single magnon with a superconducting qubit, *Science* **367**, 425 (2020).
- [19] H. Y. Yuan, Y. Cao, A. Kamra, R. A. Duine, and P. Yan, Quantum magnonics: When magnon spintronics meets quantum information science, *Phys. Rep.* **965**, 1 (2022).
- [20] Z. Li, M. Ma, Z. Chen, K. Xie, and F. Ma, Interaction between magnon and skyrmion: Toward quantum magnonics, *J. Appl. Phys.* **132**, 210702 (2022).
- [21] D. Xu, X.-K. Gu, H.-K. Li, Y.-C. Weng, Y.-P. Wang, J. Li, H. Wang, S.-Y. Zhu, and J. Q. You, Quantum control of a single magnon in a macroscopic spin system, *Phys. Rev. Lett.* **130**, 193603 (2023).
- [22] F.-X. Sun, S.-S. Zheng, Y. Xiao, Q. Gong, Q. He,

- and K. Xia, Remote Generation of Magnon Schrödinger Cat State via Magnon-Photon Entanglement, *Phys. Rev. Lett.* **127**, 087203 (2021).
- [23] M. Eschrig, Spin-polarized supercurrents for spintronics: a review of current progress, *Rep. Prog. Phys.* **78**, 104501 (2015).
- [24] J. Linder and J. W. A. Robinson, Superconducting spintronics, *Nat. Phys.* **11**, 307 (2015).
- [25] F. S. Bergeret, M. Silaev, P. Virtanen, and T. T. Heikkilä, Colloquium: Nonequilibrium effects in superconductors with a spin-splitting field, *Rev. Mod. Phys.* **90**, 041001 (2018).
- [26] Y. Yao, R. Cai, T. Yu, Y. Ma, W. Xing, Y. Ji, X. C. Xie, S.-H. Yang, and W. Han, Giant oscillatory Gilbert damping in superconductor-ferromagnet-superconductor junctions, *Sci. Adv.* **7**, eabh3686 (2021).
- [27] M. Amundsen, J. Linder, J. W. A. Robinson, I. Žutić, and N. Banerjee, Colloquium: Spin-orbit effects in superconducting hybrid structures, *Rev. Mod. Phys.* (2024).
- [28] T. Yu, M. Claassen, D. M. Kennes, and M. A. Sentef, Optical manipulation of domains in chiral topological superconductors, *Phys. Rev. Research* **3**, 013253 (2021).
- [29] B. Z. Rameshti, S. V. Kusminskiy, J. A. Haigh, K. Usami, D. Lachance-Quirion, Y. Nakamura, C.-M. Hu, H. X. Tang, G. E. W. Bauer, and Y. M. Blanter, Cavity magnonics, *Phys. Rep.* **979**, 1 (2022).
- [30] R. Cai, I. Žutić, and W. Han, Superconductor/Ferromagnet Heterostructures: A Platform for Superconducting Spintronics and Quantum Computation, *Adv. Quantum Technol.* **6**, 2200080 (2023).
- [31] K. M. D. Hals, M. Schechter, and M. S. Rudner, Composite Topological Excitations in Ferromagnet-Superconductor Heterostructures, *Phys. Rev. Lett.* **117**, 017001 (2016).
- [32] O. V. Dobrovolskiy, R. Sachser, T. Brächer, T. Böttcher, V. V. Kruglyak, R. V. Vovk, V. A. Shklovskij, M. Huth, B. Hillebrands, and A. V. Chumak, Magnon-fluxon interaction in a ferromagnet/superconductor heterostructure, *Nat. Phys.* **15**, 477 (2019).
- [33] T. Yu and G. E. W. Bauer, Efficient Gating of Magnons by Proximity Superconductors, *Phys. Rev. Lett.* **129**, 117201 (2022).
- [34] M. A. Kuznetsov and A. A. Fraerman, Temperature-sensitive spin-wave nonreciprocity induced by interlayer dipolar coupling in ferromagnet/paramagnet and ferromagnet/superconductor hybrid systems, *Phys. Rev. B* **105**, 214401 (2022).
- [35] M. Borst, P. H. Vree, A. Lowther, A. Teepe, S. Kurdi, I. Bertelli, B. G. Simon, Y. M. Blanter, and T. van der Sar, Observation and control of hybrid spin-wave-Meissner-current transport modes, *Science* **382**, 430 (2023).
- [36] I. A. Golovchanskiy, N. N. Abramov, V. S. Stolyarov, V. V. Bolginov, V. V. Ryazanov, A. A. Golubov, and A. V. Ustinov, Ferromagnet/Superconductor Hybridization for Magnonic Applications, *Adv. Funct. Mater.* **28**, 1802375 (2018).
- [37] I. A. Golovchanskiy, N. N. Abramov, V. S. Stolyarov, V. V. Ryazanov, A. A. Golubov, and A. V. Ustinov, Modified dispersion law for spin waves coupled to a superconductor, *J. Appl. Phys.* **124**, 233903 (2018).
- [38] I. A. Golovchanskiy, N. N. Abramov, V. S. Stolyarov, P. S. Dzhumaev, O. V. Emelyanova, A. A. Golubov, V. V. Ryazanov, and A. V. Ustinov, Ferromagnet/Superconductor Hybrid Magnonic Metamaterials, *Adv. Sci.* **6**, 1900435 (2019).
- [39] I. A. Golovchanskiy, N. N. Abramov, V. S. Stolyarov, A. A. Golubov, V. V. Ryazanov, and A. V. Ustinov, Nonlinear spin waves in ferromagnetic/superconductor hybrids, *J. Appl. Phys.* **127**, 093903 (2020).
- [40] A. Ghirri, C. Bonizzoni, M. Maksutoglu, and M. Afromonte, Interplay between magnetism and superconductivity in a hybrid magnon-photon bilayer system, arXiv:2312.02785.
- [41] L.-L. Li, Y.-L. Zhao, X.-X. Zhang, and Y. Sun, Possible evidence for spin-transfer torque induced by spin-triplet supercurrents, *Chin. Phys. Lett.* **35**, 077401 (2018).
- [42] K.-R. Jeon, C. Ciccarelli, H. Kurebayashi, L. F. Cohen, X. Montiel, M. Eschrig, T. Wagner, S. Komori, A. Srivastava, J. W. A. Robinson, and M. G. Blamire, Effect of Meissner Screening and Trapped Magnetic Flux on Magnetization Dynamics in Thick Nb/Ni₈₀Fe₂₀/Nb Trilayers, *Phys. Rev. Appl.* **11**, 014061 (2019).
- [43] I. A. Golovchanskiy, N. N. Abramov, V. S. Stolyarov, V. I. Chichkov, M. Silaev, I. V. Shchetinin, A. A. Golubov, V. V. Ryazanov, A. V. Ustinov, and M. Y. Kupriyanov, Magnetization Dynamics in Proximity-Coupled Superconductor-Ferromagnet-Superconductor Multilayers, *Phys. Rev. Appl.* **14**, 024086 (2020).
- [44] S. V. Mironov and A. I. Buzdin, Giant demagnetization effects induced by superconducting films, *Appl. Phys. Lett.* **119**, 102601 (2021).
- [45] M. Silaev, Anderson-Higgs Mass of Magnons in Superconductor-Ferromagnet-Superconductor Systems, *Phys. Rev. Appl.* **18**, L061004 (2022).
- [46] X.-H. Zhou and T. Yu, Gating ferromagnetic resonance of magnetic insulators by superconductors via modulating electric field radiation, *Phys. Rev. B* **108**, 144405 (2023).
- [47] M. P. Tu, K. Mbaye, L. Wartski, and J. Halbritter, rf characterization of thermally diffused superconducting niobium nitride, *J. Appl. Phys.* **63**, 4586 (1988).
- [48] A. Kawakami, Y. Uzawa, and Z. Wang, Frequency dependence of penetration depth for epitaxial NbN thin films at 0.1–1.1 THz, *Phys. C* **412**, 1455 (2004).
- [49] T. Shapoval, H. Stopfel, S. Haindl, J. Engelmann, D. S. Inosov, B. Holzapfel, V. Neu, and L. Schultz, Quantitative assessment of pinning forces and magnetic penetration depth in NbN thin films from complementary magnetic force microscopy and transport measurements, *Phys. Rev. B* **83**, 214517 (2011).
- [50] J. D. Jackson, *Classical Electrodynamics* (Wiley, New York, 1998).
- [51] J. R. Schrieffer, *Theory of Superconductivity*, (W. A. Benjamin, New York, 1964).
- [52] Supplemental Material [...] for the general solution of the radiated electric and magnetic fields by spin waves of arbitrary \mathbf{k} .
- [53] L. D. Landau and E. M. Lifshitz, *Electrodynamics of Continuous Media*, 2nd edn. (ButterworthHeinemann, Oxford, 1984).
- [54] L. R. Walker, Magnetostatic Modes in Ferromagnetic Resonance, *Phys. Rev.* **105**, 390 (1957).
- [55] T. Yu, J. Zou, B. W. Zeng, J. W. Rao, and K. Xia, Non-Hermitian topological magnonics, *Phys. Rep.* **1062**, 1 (2024).
- [56] S. Knauer, K. Davidková, D. Schmoll, R. O. Serha, A. Voronov, Q. Wang, R. Verba, O. V. Dobrovolskiy, M. Lindner, T. Reimann, C. Dubs, M. Urbánek, and A. V.

- Chumak, Propagating spin-wave spectroscopy in a liquid-phase epitaxial nanometer-thick YIG film at millikelvin temperatures, *J. Appl. Phys.* **133**, 143905 (2023).
- [57] M. A. W. Schoen, D. Thonig, M. L. Schneider, T. J. Silva, H. T. Nembach, O. Eriksson, O. Karis, and J. M. Shaw, Ultra-low magnetic damping of a metallic ferromagnet, *Nat. Phys.* **12**, 839 (2016).
- [58] H. Wang, R. Yuan, Y. Zhou, Y. Zhang, J. Chen, S. Liu, H. Jia, D. Yu, J.-P. Ansermet, C. Song, and H. Yu, Long-Distance Coherent Propagation of High-Velocity Antiferromagnetic Spin Waves, *Phys. Rev. Lett.* **130**, 096701 (2023).
- [59] Y. Sun, F. Meng, C. Lee, A. Soll, H. Zhang, R. Ramesh, J. Yao, Z. Sofer, and J. Orenstein, Dipolar spin wave packet transport in a van der Waals antiferromagnet, *Nat. Phys.* (2024).
- [60] D. B. Fischbach, Diamagnetic Susceptibility of Pyrolytic Graphite, *Phys. Rev.* **123**, 1613 (1961).
- [61] Y. Fuseya, M. Ogata, and H. Fukuyama, Transport Properties and Diamagnetism of Dirac Electrons in Bismuth, *J. Phys. Soc. Jpn.* **84**, 012001 (2015).